

# Hysteresis loop measurements in rare-earth based permanent magnets: the role of applied field rate and sample geometry

C. BEATRICE, O. BOTTAUSCIO, F. FIORILLO\*, E. PATROI<sup>a</sup>

*Istituto Nazionale di Ricerca Metrologica (INRIM), Torino, Italy*

*<sup>b</sup>ICPE-CA Advanced Research Institute for Electrical Engineering, Bucharest, Romania*

Methods currently employed in the characterization of hard magnets are briefly discussed and the challenges posed by the precise measurement of the hysteresis loop and its parameters in rare-earth based permanent magnets are stressed. It is shown that fast and reliable measurements can be performed using the Pulsed Field Magnetometer method, exploiting either the magnetometric or the fluxmetric approach. Full assessment of the obtained results calls for appraisal of the dynamic phenomena engendered by the fast changing applied field. Besides the ubiquitous magnetic aftereffect, eddy currents may lead to loop swelling in sintered rare-earth based samples. It is demonstrated that the role of eddy currents can be accounted for and the quasi-static hysteresis loop can be retrieved by simple analytical formulation.

(Received January 25, 2007; accepted February 28, 2007)

*Keywords:* Permanent magnets, Magnetic measurements, Pulsed Field Magnetometer, Eddy currents, Magnetic aftereffect

## 1. Introduction

The full characterization of rare-earth based permanent magnets can reveal a demanding task. Coercivities in excess of  $2 \cdot 10^6$  -  $3 \cdot 10^6$  A/m and very high saturation fields can make the conventional closed-circuit measuring methods based on the use of electromagnets unreliable and incomplete. Magnetic saturation of the pole faces may in fact occur well before full magnetization reversal is achieved, resulting into obvious limitations and inhomogeneities of applied field and sample magnetization [1]. With typical coercive fields (say around  $1 \cdot 10^6$  A/m) one can actually determine the demagnetization curve along the second quadrant, following passage through the saturated state upon separate application of a strong field transient [2]. But a comprehensive characterization of extra-hard magnets would possibly call for open sample methods, with the exciting field generated by means of superconducting solenoids. This is a typical laboratory scale solution, with unlikely applications in the conventional quality control of industrial products. Much interest has therefore been attached in recent times to the development of characterization methods where the required exciting field strength is obtained using the very same pulsed field apparatus applied in the standard magnetizing and demagnetizing procedures of permanent magnets [3-5]. In this paper we briefly recall the basic features of the methods conventionally applied in the characterization of the permanent magnets, with attention devoted to the special problems posed by the determination of the hysteresis loop properties of the extra-hard rare-earth based materials. We focus our attention on the Pulsed Field Magnetometer (PFM) technique and its application to the measurement of the hysteresis loop through either magnetometric or fluxmetric measuring techniques. Since the applied field rate in the PFM method is orders of magnitude higher than with the

other methods, discrepant results may be put in evidence. It is the general problem of dynamic versus quasi-static magnetic behavior, the latter being the one eventually aimed at. In assessing the dynamic effects, we shall distinguish between the role of magnetic viscosity (thermal fluctuation aftereffect) and that of eddy currents. We will show that magnetic viscosity always leads in a PFM characterized sample to a measured coercive field  $H_c$  a few percent higher than the value resulting from measurements made under a slowly varying exciting field. Such a small increase is, to a good approximation, proportionally related to the value of  $H_c$ . Further hysteresis loop swelling by eddy currents may take place in sintered rare-earth based samples. For the case discussed here, where the magnetization period is  $T = 11$  ms, eddy current effects become detectable in Nd-Fe-B cylindrical samples with diameter  $D \gg 10$  mm. It is demonstrated that by simple analytical formulation, including demagnetizing effects, the quasi-static hysteresis loop can be retrieved. It is therefore concluded that accurate and complete characterization of hard and extra hard magnets can be afforded by the PFM method. The equivalence of magnetometric and fluxmetric approaches to the measurement of the sample magnetization is additionally shown, but for the appearance of a soft transition on the demagnetization curve, whose contribution increases with decreasing the sample volume.

## 2. Characterization of extra-hard magnets: electromagnet, vibrating sample, extraction, and pulsed field magnetometers

The standard test methods for permanent magnets call for the use of a closed magnetic circuit, with an electromagnet playing at the same time the role of field

source and flux-closing structure. The field is made to cyclically evolve, at a frequency of the order of some  $10^2$  Hz, in a continuous fashion between symmetric peak values, according to the conventional hysteresisgraph procedure [2, 6]. They are absolute measuring methods, traceable to the base SI units and solidly assessed by international comparisons [7], but they are difficult to apply in rare-earth based (e.g. Nd-Fe-B and Sm-Co) magnets and become somewhat unreliable for coercivities exceeding  $1.5 - 2 \cdot 10^6$  A/m. In fact, in order to achieve and overcome such field strengths in the gap, the pole caps may approach magnetic saturation, leading to poor flux closure and inhomogeneous effective field and induction in the sample. A cumbersome measuring procedure is also required, with pre-emptive separate application of a saturating field to the sample, complicated handling of sample and sensing coils during insertion between the pole faces of the electromagnet, and long integration times.

Hard magnets can be accurately characterized as open samples. Contrary to the soft magnetic materials, they are little sensitive to the environmental fields and the correction for the demagnetizing field does not pose special problems in regularly shaped (e.g. spherical) samples. The hysteresis loop measurement is typically accomplished by determining the total magnetic moment of the test specimen as a function of the applied field, whose strength is changed in a step-like fashion. At any step the magnetic moment is measured by intercepting the extra flux lines emanated by the sample and discriminating them against the applied field lines. In the Vibrating Sample Magnetometer (VSM) an alternating motion is imparted to the sample and the variation of the flux linked with a pickup coil is detected. The coil is endowed with a suitably high and uniform spatial gradient of its constant at the sample position. In the Extraction Magnetometer (EM) a flux variation proportional to the magnetic moment is detected by removing the sample from a position where flux linkage with a search coil is maximum to a distant place, where linkage is zero. Both methods exploit the reciprocity principle, which, by virtue of the equivalence

between magnetic dipole and current loop and the concept of mutual inductance, states that the flux  $\Phi$  linked to a search coil in the presence of a magnetic dipole of moment  $\mathbf{m}$  located in a point of coordinates  $(x, y, z)$  is

$$\Phi = \mathbf{k}(x, y, z) \cdot \mathbf{m} = k_x(x, y, z)m_x + k_y(x, y, z)m_y + k_z(x, y, z)m_z \quad (1)$$

where  $\mathbf{k}(x, y, z)$  is the coil constant, that is the ratio  $\mathbf{k}(x, y, z) = \mathbf{B}(x, y, z) / i_s$  between the flux density generated by the coil at the position occupied by the point-like dipole when a current  $i_s$  is made to circulate in it. The magnetization  $\mathbf{M}$  is obtained, in a uniformly magnetized sample of volume  $V$ , from the measured magnetic moment as  $\mathbf{M} = \mathbf{m} / V$ . The uniform magnetization and point-like dipole conditions are naturally fulfilled in small spherical test specimens. With typical size and arrangement of superconducting solenoids and pickup coils, the convenient sample diameter is of the order of a few millimeters. Recent examples of VSM and EM approaches to permanent magnet characterization by use of superconducting field sources are reported in Refs. [8, 9]. Fig. 1a provides a sketchy view of a VSM setup. The sample, made to oscillate along the  $z$ -axis, is placed at the center of an inverse Helmholtz pair (coil radius  $a$ ), which intercepts its stray field lines and generates an instantaneous voltage

$$u(t) = d\Phi / dt = m \frac{d}{dz} k(z) \cdot \dot{z} = mg(z) \cdot \dot{z} \quad (2),$$

where  $g(z) = dk(z) / dz$  is called sensitivity function of the pickup coil. An inverse Helmholtz pair with distance between the coils  $d = \sqrt{3}a$  provides maximum linearity of the response. The typical vibration frequency may range between a few Hz and some hundred Hz.

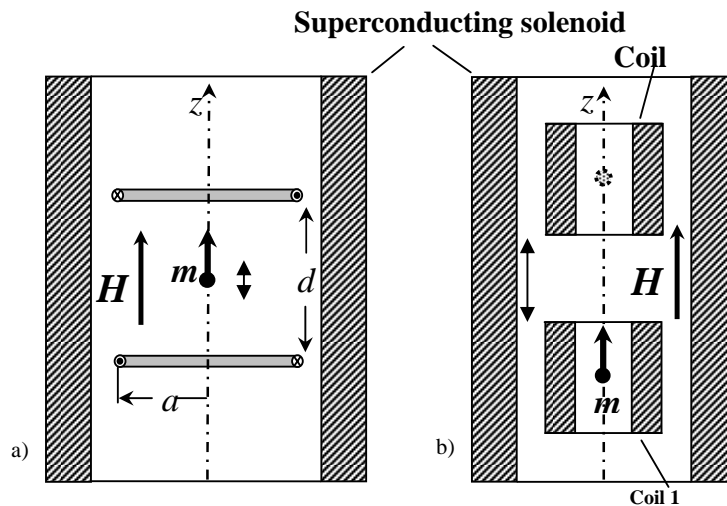


Fig. 1. Schematic arrangement and working principle of a Vibrating Sample Magnetometer (a) and an Extraction Magnetometer (b) using a superconducting solenoid. These devices, suitable for characterization of the rare-earth based permanent magnets, call for small test specimens, typically prepared as a few mm diameter spheres.

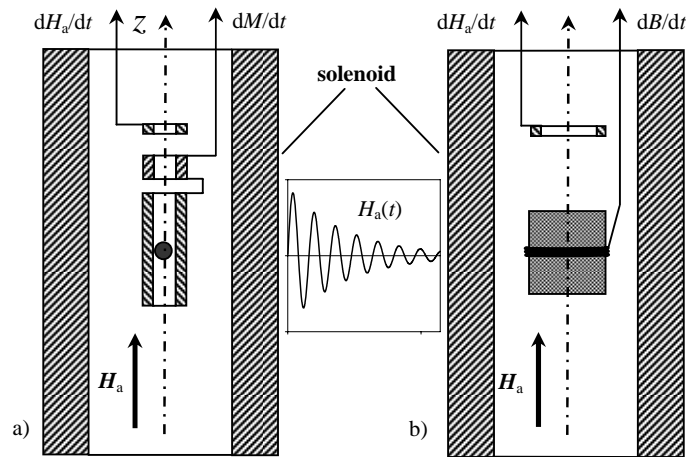


Fig. 2. Characterization of permanent magnets with the Pulsed Field Magnetometer in the oscillatory transient mode. a) Moment measuring (magnetometric) method (small spherical samples). b) Fluxmetric method (cylindrical/parallelepipedic samples).

Fig.1b illustrates an EM arrangement that can be suitably adopted for testing extra-hard magnets. The measuring procedure consists in the displacement of the specimen from the center of coil 1 to the center of the identical coil 2, which is connected in series opposition. The two coils are located sufficiently far apart to avoid any cross-linkage of the flux when the sample is in its rest position (the center of the coil). If the coil constant at such position is  $k_z$ , the flux linked at start is  $\Phi_1 = k_z m$ . At the end of the sample travel it is  $\Phi_2 = -k_z m$ , so that, by integrating the resulting voltage pulse we obtain the flux variation  $\Delta\Phi = 2k_z m$ .

VSM and EM can be highly sensitive devices, but they do not provide absolute measurements. This is due to the image effect, a distortion by the diamagnetic walls of the superconducting solenoid of the field lines emerging from the sample, which can be figured out according to the notional idea of an image dipole [10]. Calibration by means of a reference sample, typically a pure Ni sphere held close to saturation by a defined high field, is therefore required. The use of small samples is, besides the obvious complications and costs associated with the application of cryogenic field sources, a drawback in the industrial environment, where the additional step of sphere grinding from samples of commercial size is unattractive for the sake of quality control and clearly inapplicable when demand exists for individual testing of the produced magnets. We will show in the following that one can also come across an appreciable size effect in rare-earth based magnets.

It has been stated that a possible way to achieve an industrially viable approach to full testing of modern extra-hard permanent magnets is by use of pulsed fields [3-5]. To this end, one can exploit the same apparatus employed in the conventional magnetizing and demagnetizing operations, that is, a large capacitor bank (typically more than 1 mF) charged to a few kV voltage and discharged in either oscillatory or non-oscillatory transient mode into a many-layer solenoid. The device used in the presently reported experiments is built around a 3.6 mF capacity, charged to a maximum voltage of 3 kV

and discharged into a solenoid of inductance  $L = 0.85$  mH (bore diameter 50 mm, length 170 mm). The resulting maximum peak field, achieved after the first quarter period in the here-adopted oscillatory mode ( $T \cong 11$  ms), is around 6 MA/m. The successive opposite peak field strength is about 25 % lower, but high enough to achieve technical saturation in the opposite direction and complete the half-loop in most cases of practical interest. One important feature of the PFM approach to magnet testing is the possibility to apply it to both small spherical samples and practically sized cylinders and parallelepipeds, switching from the previously described magnetometric method to the conventional fluxmetric method. The corresponding arrangements are schematically illustrated in Figs. 2a and 2b, respectively. The pickup coil in Fig. 2a is a 20 mm long solenoid, which can accommodate spherical test specimens up to about 4 mm diameter, the uniformity of the  $k_z$  constant over this distance being better than 0.3 %. The flux linked with such a coil at a given instant of time under the applied field  $H_a$  is  $\Phi = \Phi_s + \Phi_a$ , the sum of the contributions from the sample magnetization  $\Phi_s = k_z MV$  and the applied field  $\Phi_a = A\mu_0 H_a$ , where  $A$  is the turn-area of the coil.  $\Phi_a$  is usually much higher than  $\Phi_s$  and it must be finely compensated by connecting in series opposition a second axial coil, located far enough from the sample to be immune from its stray field. The applied field is measured by means of a further axial coil, previously calibrated inside a reference source [12]. The detected signals, proportional to  $dM/dt$  and  $dH_a/dt$ , respectively, are amplified, sampled at 800 kHz, and A/D converted at 14 bit resolution by means of a VXI acquisition setup. The measuring procedure is completed with the usual mathematical operations on the converted signal, including integration, drift correction, and background subtraction, all performed in a VEE software environment. To be stressed that the residual air flux leaking into the detected signal in spite of compensation is mathematically eliminated after two separate identical experiments, with and without the sample. The effective field is obtained, after correction for the demagnetizing field, as

$H_{\text{eff}} = H_a - M/3$ . Although absolute measurements are possible, better measuring accuracy is obtained by calibrating the pickup coil by means of a reference sample. Such a sample cannot be the previously mentioned pure Ni sphere, because under typical pulse durations the eddy current effects would impair the measuring accuracy. A Ba ferrite spherical sample (diameter 3 mm), whose magnetic moment at a field of  $8 \cdot 10^5$  A/m has been precisely determined in a calibrated VSM setup, has been employed for the determination of the coil constant  $k_z$ , which is obtained with an estimated uncertainty  $2\sigma$  around  $\pm 0.5\%$ .

The relatively simpler fluxmetric arrangement in Fig. 2b, with its standard hysteresisgraph approach, is what we need in principle with samples of industrial size. But the fast oscillation rate of the applied field is conducive to dynamic effects, while non-spherical sample shape implies non-uniform demagnetizing field. We shall provide in the following, by combination of theory and experiment, a rationale for the retrieval of the intrinsic DC behavior of rare-earth based permanent magnets starting from PFM experiments, by taking at face value the role of demagnetizing field, magnetic aftereffect, and eddy currents.

### 3. Experimental results: PFM versus closed circuit, VSM and EM methods

In order to elucidate the potential of the PFM method for accurate and application-prone measurements in permanent magnets, a wide-ranging comparison with other measuring methods has been carried out. This implied a variety of test sample sizes (from 2 mm diameter spheres to 28.5 mm diameter cylinders) and impressed magnetization rates (from about  $10^{-3}$  Ts $^{-1}$  to some  $10^3$  Ts $^{-1}$ ). The quantitative assessment of the dynamic effects is indeed central to the general acceptance of the PFM method in the laboratory and the industrial practice, because sintered rare-earth based magnets display metallic conductivity (for example  $\sigma = 6.95 \cdot 10^5$   $\Omega^{-1}\text{m}^{-1}$  in Nd-Fe-B and  $\sigma = 1.65 \cdot 10^6$   $\Omega^{-1}\text{m}^{-1}$  in SmCo $_5$ ). A substantial effort has therefore been spent in the literature for the experimental and numerical appraisal of eddy current effects and their correction [3, 13]. It has been remarked, however, that magnetic viscosity due to the thermal fluctuation aftereffect would enter into play and be an additional source of discrepancy between the results obtained by the PFM and the other measuring methods [14]. This can be directly verified by testing either non-conducting materials (e.g. hard ferrites and bonded samples) or small sintered samples, where eddy-current effects are irrelevant. The latter case is illustrated in Figs. 3a and 3b, where comparison is made between the hysteresis loops determined on a same spherical sample (diameter  $D = 3.53$  mm) by the slow EM method ( $T = 4500$  s) and the fast PFM method ( $T = 11$  ms). The impressed induction rates are, along the steep part of the hysteresis loop,  $(dB/dt)_{\text{EM}} \sim 2 \cdot 10^{-3}$  Ts $^{-1}$  and  $(dB/dt)_{\text{PFM}} \sim 5 \cdot 10^3$  Ts $^{-1}$ , respectively. It is immediately verified that the extra contribution  $\Delta H_c$  to the coercive field brought about by the six orders of magnitude increase of the induction rate in the PFM tested sample cannot derive from eddy currents. For a given induction rate, we can in fact express the counterfield generated by eddy

currents in a sphere of diameter  $D$  and conductivity  $\sigma$  as  $H_{\text{eddy}} \cong (\sigma D^2/40) \cdot dB/dt$ , which provides, for the PFM experiment in Fig. 3,  $H_{\text{eddy}} \cong 1020$  A/m. This quantity is negligible compared to experimental value  $\Delta H_c \sim 1.6 \cdot 10^5$  A/m. The loop enlargement at high field rates is related to the magnetic aftereffect. The magnetization process in hard magnets is a thermally aided process, the system being driven by thermal agitation towards the thermodynamic equilibrium if given the time to do so. One can phenomenologically describe thermal relaxation by assuming that the magnetization can vary with time as though it were under the action of an internal random field  $H_r(t)$  adding to the external field and increasing with time  $t$  according to a logarithmic law  $H_r(t) = H_f \ln(1+t/\tau_0)$ , where  $H_f$  is called fluctuation field and the time constant  $\tau_0$ , the inverse of an attempt frequency for overcoming the energy barriers hindering the local magnetization reversals, is typically assumed to be of the order of  $10^{-10}$  s [15]. We might therefore expect that, grossly lacking the aid of  $H_r(t)$ , an excess field shall be required under fast magnetization reversal with respect to the case of slow reversal. This effect depends on the nature of the material, but, contrary the eddy currents, it is independent of conductivity and sample size. It can therefore be invoked to explain the different coercivities found by PFM and the other methods also in insulating Ba ferrites and bonded Nd-Fe-B samples. Representative results obtained in these two materials, tested both as spherical and cylindrical samples, are shown in Figs. 4a and 4b.

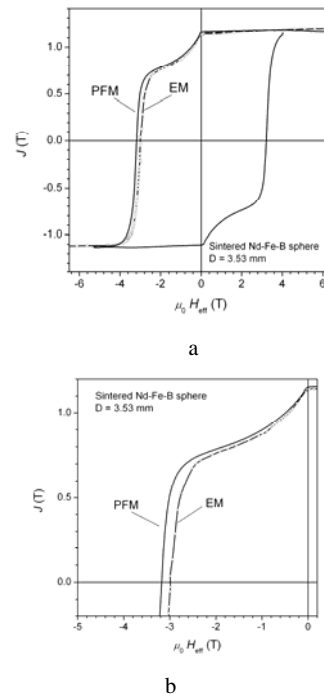


Fig. 3. Hysteresis loop in sintered Nd-Fe-B (3.53 mm diameter spherical sample) measured with the aid of a superconducting field source in an Extraction Magnetometer (EM) and with a Pulsed Field Magnetometer (PFM). The measuring temperature is 23 °C. The magnetization period is changed from  $T = 4500$  s to  $T = 11$  ms on passing from EM to PFM. a) Full loop. b) Demagnetization curve along the second quadrant.

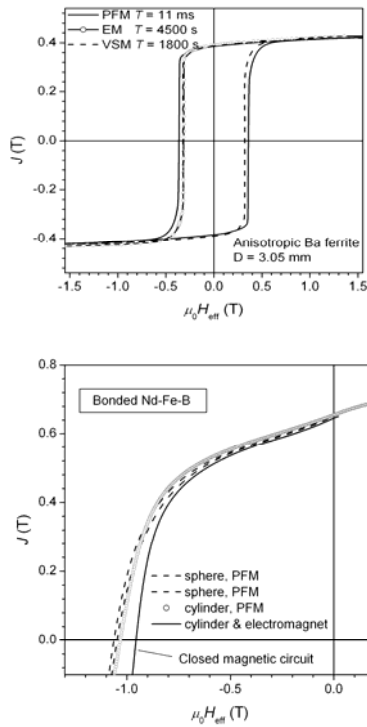


Fig. 4. a) Hysteresis loop measured in an anisotropic Ba ferrite spherical sample with three different methods: PFM, EM, VSM. b) Demagnetization curves in bonded Nd-Fe-B. This material is tested as a cylindrical sample (diameter  $D = 25$  mm, height  $h = 10.5$  mm) with both the standard closed circuit method ( $T \cong 100$  s) and the PFM method. Spherical samples are then obtained out of the cylinder and tested again in the PFM setup.

A full scale comparison of the results obtained on the same samples with the PFM method and the slow methods shows that the dependence of the experimental  $\Delta H_c$  on the coercive field  $H_c$  of the investigated material can be approximately described by a linear law. This is illustrated in Fig. 5, where the relationship  $\Delta H_c = 7 \cdot 10^{-2} H_c$  appears to agree to a good extent with the measurements performed on isotropic and anisotropic Ba ferrites, bonded and sintered Nd-Fe-B, and sintered  $\text{SmCo}_5$ . Assuming  $H_f(t_2 - t_1) = H_f \ln(t_2/t_1) = \Delta H_c$ , with  $t_2/t_1 = 3.5 \cdot 10^5$ , we obtain for the fluctuation field  $H_f = 5.5 \cdot 10^{-3} H_c$ . To note that the classical relationship between  $H_f$  and  $H_c$ , as derived from aftereffect experiments, is of the type  $H_f \propto H_c^n$ , with  $n = 1.35 - 1.5$  [16, 17]. On the other hand, Grössinger et al. have obtained from PFM experiments that  $H_f$  can increase linearly with  $H_c$  in giant magnetic viscosity  $\text{SmCo}_{5-x}\text{Cu}_x$  alloys [14].

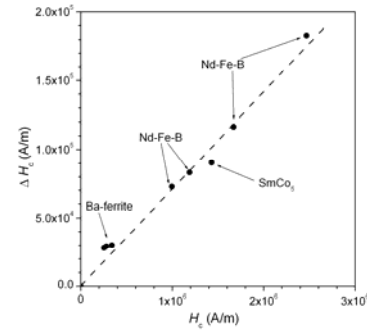


Fig. 5. The excess coercivity  $\Delta H_c$  exhibited by the PFM hysteresis loops in eddy current free samples is related to the thermal fluctuation after effect. The experiments carried out in different materials point to a linear dependence of  $\Delta H_c$ , that is the fluctuation field  $H_f$ , on the coercive field  $H_c$ . It is found  $H_f = 5.5 \cdot 10^{-3} H_c$ .

#### 4. Role of eddy currents and retrieval of the quasi-static hysteresis loop

The so far discussed PFM results refer to eddy current free samples. But, given the metallic character of the sintered rare-earth base magnets, such effects may be relevant in industrially sized samples. Their appraisal and the corresponding recovery of the quasi-static hysteresis loop have been conducted in the literature either by empirical methods (the so-called  $f/2f$  approach [4]) or by finite-element modeling of the transient field distribution in cylindrical samples [13, 18]. While the  $f/2f$  method requires a substantial piece of equipment and ignores any contribution from magnetic viscosity, the general user may not easily implement the numerical methods. We have verified that the PFM loops obtained with the previously sketched conventional equipment ( $T \cong 11$  ms, maximum field 6 MA/m) in sintered Nd-Fe-B cylindrical samples do not require correction for eddy currents below about 10 mm diameter. It is additionally shown that, whenever eddy current effects are to be considered, a simple analytical formulation for the eddy current counterfield, coupled with the correction for magnetic viscosity and demagnetizing effect, permits one to retrieve the quasi-static intrinsic hysteresis loop of the material. The demagnetizing field  $H_d$  in cylinders is non-homogeneous and the induction is advantageously measured by means of a narrow coil located at the sample midplane, perpendicular to the axis (see Fig. 2b). Here the area-averaged demagnetizing factor is defined as  $\langle N_d \rangle = \int_S H_d dS / M$ . To simplify the calculation, the sample magnetization is assumed to be uniform (susceptibility  $\chi = 0$ ). Consequently,  $\langle N_d \rangle$  can be calculated either by analytical method or directly retrieved by tabulated data for any aspect ratio of the sample [19]. The measurement provides, after integration of the signals detected by the  $H$ -winding and the secondary winding, the

applied field  $H_a(t)$  and the sample induction  $B(t)$ . If eddy current effects are disregarded, the effective field and the magnetic polarization are obtained as

$$J = (B - \mu_0 H_a) / (1 - \langle N_d \rangle) \quad H_{\text{eff}} = H_a - (\langle N_d \rangle / \mu_0) J \quad (3)$$

In Fig. 6 we apply Eq. (3) to the PFM fluxmetric measurements carried out in narrow ( $D = 6$  mm,  $h = 20$  mm) and large ( $D = 28.5$  mm,  $h = 10$  mm) Nd-Fe-B cylindrical samples. The loop obtained by magnetometric measurement on a small sphere ground out of the narrow cylinder is also shown. The agreement between the two measuring methods under the appropriate sample geometry is proved, but for the different breadth of the soft transition region observed beyond the remanence point. This effect expectedly occurs because of the existence of a soft layer at the sample surface, the smaller the sample the stronger its contribution. Loop swelling by the eddy current counterfield  $H_{\text{eddy}}$  is apparent in the large diameter sample. We wish to correct for such an extra field and, by additional compensation of the magnetic viscosity field  $\Delta H_c$ , to retrieve the quasi-static hysteresis loop of the material.

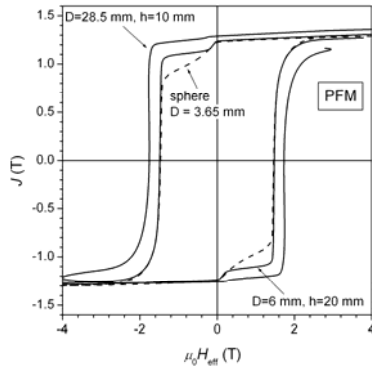


Fig. 6. A narrow cylindrical ( $D = 6$  mm,  $h = 10.5$  mm) sample is tested by fluxmetric PFM (Fig. 2b) and the ( $J$ ,  $H_{\text{eff}}$ ) hysteresis loop is obtained applying Eq. (3). A small spherical sample is then ground out of it and tested by magnetometric PFM (Fig. 2a). Loop swelling by eddy currents is apparent when a 28.5 mm diameter cylindrical sample is measured.

In order to compensate for the eddy current effect on the enlarged loop in Fig. 6 we need to calculate at any instant of time the field  $H_{\text{eddy}}$ , exploiting the knowledge of the induction derivative  $dB/dt$ , directly provided by the experiment. We assume that at the sample midplane  $dB/dt$  is uniform upon the whole cross-section, so that Eq. (3) becomes

$$J = (B - \mu_0 H_a + \mu_0 \langle H_{\text{eddy}} \rangle) / (1 - \langle N_d \rangle) \\ H_{\text{eff}} = H_a - (\langle N_d \rangle / \mu_0) J - \langle H_{\text{eddy}} \rangle \quad (4).$$

The brackets in  $\langle H_{\text{eddy}} \rangle$  indicate averaging over the cross-sectional area of the sample. We find  $\langle H_{\text{eddy}}(t) \rangle$  by a classical calculation (continuous magnetization process in space and time), by integrating the contributions of the current rings and averaging upon the midplane cross-sectional area. For a cylinder of height  $h$  we find

$$\langle H_{\text{eddy}}(t) \rangle = \frac{\sigma}{R^2} \cdot \frac{dB}{dt} \cdot \int_0^R \frac{(R^2 - r^2)r}{\sqrt{1 + (2R/h)^2} + \sqrt{1 + (2r/h)^2}} dr \quad (5),$$

which, in high aspect ratio cylinders ( $h \gg R$ ) reduces to  $H_{\text{eddy}} \cong (\sigma D^2 / 32) \cdot dB/dt$ .

An example of PFM hysteresis loop obtained in a large diameter sintered Nd-Fe-B sample is shown in Fig. 7, together with its eddy current field correction by Eqs. (4) and (5). The final calculated loop is compared in the second quadrant with the quasi-static demagnetization curve determined by the conventional closed circuit hysteresisgraph method. It is noted that, after further correction for the magnetic viscosity field  $\Delta H_c$ , known from the experimental law shown in Fig. 5, the quasi-static hysteresis loop is recovered with good approximation.

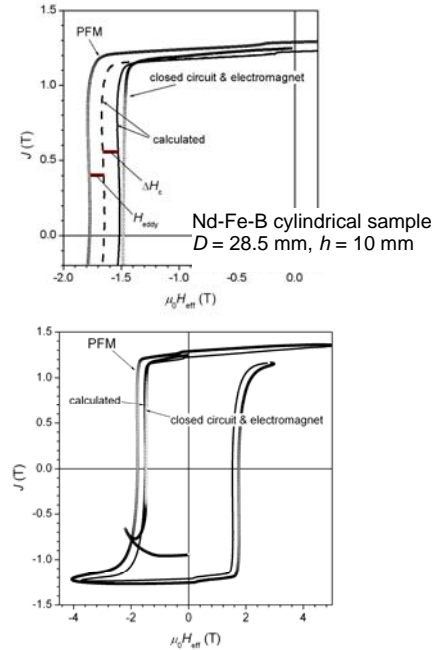


Fig. 7. A 28.5 mm diameter Nd-Fe-B sintered sample is tested both by PFM and closed circuit method ( $T = 11$  ms versus  $T = 100$  s). The figures show the experimental and the corrected loops. The demagnetization curve in the second quadrant is shown in a). The dashed line is obtained from the PFM loop after correction for the eddy current field by Eqs. (4) and (5). Further correction for the viscosity field  $\Delta H_c$  leads to the final loop (solid lines in a) and b)).

#### 4. Conclusions

The measurement of the hysteresis loop in extra-hard rare-earth based permanent magnets by the Pulsed Field Magnetometer is an affordable alternative to the methods exploiting superconducting field sources. The very short magnetization period, of the order of a few ms, imposes certain corrections on the as-obtained loops, in order to retrieve the quasi-static hysteresis loop. We have shown that with a period around 10 ms, magnetic viscosity effects are responsible for an increase of the coercive field with respect to the quasi-static case of the order of 7 % in all materials, that is, proportional to the actual value of the coercive field. Eddy current related swelling of the hysteresis loop is additionally observed in large-sized sintered magnets (e.g. Nd-Fe-B and Sm-Co). A simple analytical approach to the eddy current fields permits one to compensate for such an effect and to recover the quasi-static loop in cylindrical samples.

#### Acknowledgments

The authors thank Dr. V. Basso for many stimulating discussions. Assistance by Laboratorio Elettrofisico (Nerviano, Italy) in the development of the pulsed field source is gratefully acknowledged.

#### References

- [1] F. Fiorillo, *Measurement and Characterization of Magnetic Materials*, Elsevier-Academic Press, Amsterdam (2004), p. 481.
- [2] IEC Standard Publication 60404-5, *Permanent Magnet (Magnetically Hard) Materials-Methods of Measurement of Magnetic Properties*, IEC Central Office, Geneva (1993).
- [3] R. Grössinger, Ch. Gigler, A. Keresztes, *IEEE Trans. Magn.*, **24**, 970 (1988).
- [4] R. Grössinger, G.W. Jewell, J. Dudding, D. Howe, *IEEE Trans. Magn.*, **29**, 2981 (1993).
- [5] P. Bretchko, R. Ludwig, *IEEE Trans. Magn.*, **36**, 2042 (2000).
- [6] ASTM Publication A977/A 977M-02, *Standard test methods for magnetic properties of high-coercivity permanent magnet materials using hysteresigraphs*, ASTM International, West Conshohocken, PA (2002).
- [7] J. Sievert, H. Ahlers, J. Lüdke, S. Siebert, L. Pareti, M. Solzi, *IEEE Trans. Magn.*, **29**, 2887 (1993).
- [8] D. Dufeu, P. Lethuillier, *Rev. Sci. Instrum.* **70**, 137 (1999).
- [9] D. Dufeu, T. Eyraud, P. Lethuillier, *Rev. Sci. Instrum.* **71**, 458 (2000).
- [10] A. Zieba, S. Foner, *Rev. Sci. Instrum.* **54**, 137 (1983).
- [11] F. Fiorillo, *ibid.*, p. 127.
- [12] F. Fiorillo, G.F. Durin, L. Rocchino, *J. Magn. Magn. Mater.* **304**, e540 (2006).
- [13] C. Golovanov, G. Reyne, G. Meunier, R. Grössinger, J. Dudding, *IEEE Trans. Magn.*, **36**, 1222 (2000).
- [14] R. Grössinger, R. Sato Turtelli, C. Téllez-Blanco, *J. Optoelectron. Adv. Mater.* **6**, 557 (2004).
- [15] L. Néel, *J. Phys. Rad.* **12**, 339 (1951).
- [16] J. C. Barbier, *Ann. Phys.* **9**, 84 (1954).
- [17] E. P. Wohlfarth, *J. Phys. F* **14**, L-155 (1984).
- [18] G. W. Jewell, D. Howe, C. Schotzko, R. Grössinger, *IEEE Trans. Magn.*, **28**, 3114 (1992).
- [19] D. X. Chen, J.A. Brug, R.B. Goldfarb, *IEEE Trans. Magn.*, **27**, 3601 (1991).

\*Corresponding author: fiorillo@inrim.it